www.nature.com/aps

Acta Pharmacologica Sinica

ARTICLE

Antiangiogenesis effect of timosaponin AIII on HUVECs in vitro and zebrafish embryos in vivo

Zhong-yan Zhou[1,2], Wai-rong Zhao[1,3], Ying Xiao[1], Xiang-ming Zhou[1], Chen Huang[2], Wen-ting Shi[1], Jing Zhang[1], Qing Ye[1], Xin-lin Chen[1] and Jing-yi Tang[1,3]

Timosaponin AIII (Timo AIII) is a natural steroidal saponin isolated from the traditional Chinese herb *Anemarrhena asphodeloides* Bge with proved effectiveness in the treatment of numerous cancers. However, whether Timo AIII suppresses tumor angiogenesis remains unclear. In the present study, we investigated the antiangiogenesis effects of Timo AIII and the underlying mechanisms in human umbilical vein endothelial cells (HUVECs) in vitro and zebrafish embryos in vivo. We showed that treatment with Timo AIII (0.5–2 μM) partially disrupted the intersegmental vessels (ISVs) and subintestinal vessels (SIVs) growth in transgenic zebrafish Tg(*fli-1a*: EGFP)^{y1}. Timo AIII (0.5–4 μM) dose-dependently inhibited VEGF-induced proliferation, migration, invasion, and tube formation of HUVECs, but these inhibitory effects were not due to its cytotoxicity. We further demonstrated that Timo AIII treatment significantly suppressed the expression of VEGF receptor (VEGFR) and the phosphorylation of Akt, MEK1/2, and ERK1/2 in HUVECs. Timo AIII treatment also significantly inhibited VEGF-triggered phosphorylation of VEGFR2, Akt, and ERK1/2 in HUVECs. Moreover, we conducted RNA-Seq and analyzed the transcriptome changes in both HUVECs and zebrafish embryos following Timo AIII treatment. The coexpression network analysis results showed that various biological processes and signaling pathways were enriched including angiogenesis, cell motility, cell adhesion, protein serine/threonine kinase activity, transmembrane signaling receptor activity, growth factor activity, etc., which was consistent with the antiangiogenesis effects of Timo AIII in HUVECs and zebrafish embryos. We conclude that the antiangiogenesis effect of Timo AIII is mediated through VEGF/PI3K/Akt/MAPK signaling cascade; Timo AIII potentially exerts antiangiogenesis effect in cancer treatment.

Keywords: Timosaponin AIII; Traditional Chinese herbal; Neovascularization; Neoplasm; VEGF/PI3K/Akt/MAPK; Transcriptome; Zebrafish; HUVECs; SU5416

Acta Pharmacologica Sinica (2020) 41:260–269; https://doi.org/10.1038/s41401-019-0291-z

INTRODUCTION

Cancer, which poses a major threat to public health worldwide, is the second leading cause of death in the USA, and the prevalence and burden of cancer continue to increase in China as well [1, 2]. Tumor angiogenesis leads to the formation of new blood vessels that transport oxygen and nutrients; this process controls tumor growth and metastasis and plays a key role in the progression of tumors [3, 4]. Tumor cells secreting angiogenic factors, such as bFGF, vascular endothelial growth factor (VEGF), TNF-α, and Hif-α, promote the proliferation, migration, and invasion of endothelial cells and initiate the growth of new blood vessels from the preexisting vasculature in tumors [5, 6]. Thus, targeting inhibition of tumor angiogenesis is considered an important therapeutic strategy in cancer patients [7].

Timosaponin AIII (Timo AIII, Fig. 1) is a natural steroidal saponin isolated from Chinese Materia Medica *Anemarrhena asphodeloides* Bge and is commonly used to treat depression, hematochezia, diabetes, cough, hemoptysis, and cardiovascular disease in traditional Chinese medicine [8, 9]. Timo AIII has multiple pharmacological activities, including antiinflammatory [10] and antiplatelet aggregation activities [11], improves learning and memory [8] and inhibits the passive cutaneous anaphylaxis reaction and pruritus [12]. Interestingly, Timo AIII induces hepatotoxicity, and this effect is protected by mangiferin, which is another component in *A. asphodeloides* Bge [13]. Moreover, Timo AIII selectively induces cell death in tumor cells but not in normal cells and has been suggested to be a novel potential anticancer compound in recent years [14, 15]. Timo AIII presents antitumor activity in various cancers, such as non-small cell lung cancer [16], pancreatic cancer [17], melanoma [18, 19], breast cancer [20], hepatocellular carcinoma [21], colon cancer [22], promyelocytic leukemia [23] and so on. In addition, Chen et al. found that Timo AIII also reverses multidrug resistance in human chronic myelogenous leukemia [24]. Various molecular mechanisms, including proapoptosis, antiproliferation, antimigration, antiinvasion, induction of ROS and ER stress and autophagy, are involved in the anticancer activity of Timo AIII [14].

[1]Longhua Hospital, Shanghai University of Traditional Chinese Medicine, Shanghai 200032, China; [2]State Key Laboratory of Quality Research in Chinese Medicine and Institute of Chinese Medical Sciences, University of Macau, Macao, China and [3]Cardiac rehabilitation Center of Longhua Hospital, Shanghai University of Traditional Chinese Medicine, Shanghai 200032, China
Correspondence: Xin-lin Chen (heal7374@163.com) or Jing-yi Tang (dr_tang@163.com)
These authors contributed equally: Zhong-yan Zhou, Wai-rong Zhao, Ying Xiao

Received: 25 February 2019 Accepted: 17 July 2019
Published online: 12 September 2019

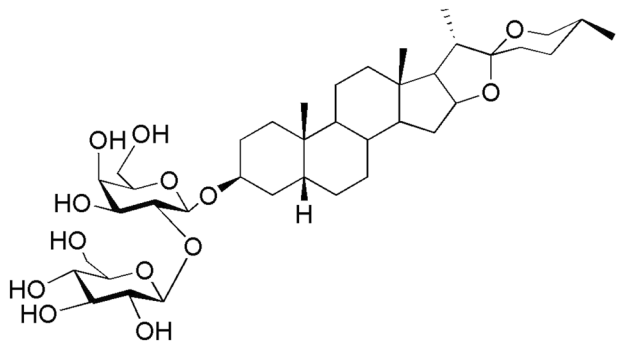

Fig. 1 Chemical structure of timosaponin AIII (Timo AIII, PubChem CID: 10628815)

However, whether Timo AIII inhibits the tumor angiogenesis process is not clear. In the present study, we explored the antiangiogenesis effect of Timo AIII and its mechanism of action using endothelial cell and zebrafish models.

MATERIALS AND METHODS

Chemicals

3-(4,5-dimethyl-thiazol-2-yl)−2,5-diphenyl tetrazolium bromide (MTT), endothelial cell growth supplement (ECGS) and heparin were purchased from Sigma Aldrich (St Louis, MO, USA). VEGF was purchased from PeproTech (Rocky Hill, NJ, USA). SU5416 was purchased from Cayman Chemical (Ann Arbor, MI, USA). Cell culture reagents were supplied by Thermo Fisher (Waltham, MA, USA). Antibodies were purchased from Cell Signaling Technology (Danvers, Massachusetts, USA). Timo AIII (purity by HPLC ≥ 98.0%) was purchased from Chengdu Must Bio-Technology Co., Ltd (Chengdu, Sichuan, China).

Ethics statement

All experiments related to zebrafish described in this study were in accordance with the Animal Experimentation Ethics Committee, Shanghai University of Traditional Chinese Medicine.

Maintenance and embryo handling of zebrafish

The transgenic zebrafish line Tg(*fli-1a*: EGFP)^{y1}, which expresses enhanced green fluorescent protein (EGFP) in endothelial cells, was kindly provided by Prof. Simon Lee from the University of Macau. Fish maintenance was performed according to the Zebrafish Handbook (Westerfield, 2007). In brief, zebrafishes were kept separately under a 14 h light and 10 h dark cycle and fed brine shrimp twice a day. Zebrafish embryos were generated by natural pair-wise mating and incubated at 28.5 °C in embryo medium. After 24 h of incubation, chorions were removed by a sharp forceps, and health development embryos were selected for later use.

Cell viability assay of human umbilical vein endothelial cells

Human umbilical vein endothelial cells (HUVECs) were purchased from American Type Cell Culture (ATCC, catalog: ATCC® CRL-1730™) and cultured in F-12K medium supplemented with 0.1 mg/mL heparin, 0.05 mg/mL ECGS, 10% (v/v) FBS and 1% penicillin/streptomycin at 37 °C in a 95% humidified incubator with 5% CO_2 in air. HUVECs were seeded at a density of 1×10^4 cells/well in a 96-well plate and preincubated until they reached 70–80% confluence. After 24 h of starvation in basal F-12K medium, HUVECs were treated with various concentrations of Timo AIII (0.5, 1, 2, 4, and 8 μM) with or without VEGF (50 ng/mL) for 24 h. HUVECs were treated with DMSO (0.1%) as a vehicle control and SU5416 (1 μM) as a positive control. The cell viability of HUVECs was tested by the MTT assay according to the manufacturer's instructions. Cell viability was expressed according to the percentage of the vehicle control.

Real-time endothelial cell proliferation analysis by an RTCA

HUVEC cell growth was detected in real time using a real-time cell analysis (RTCA) system named xCELLigence (ACEABIO S16, Hangzhou, China). HUVECs were seeded at a density of 0.5×10^4 cells/well in a specified 16-well plate. HUVECs were settled for 30 min before being placed in an xCELLigence instrument at 37 °C in a 95% humidified incubator with 5% CO_2 in air. After incubation for 24 h, HUVECs were treated with VEGF (50 ng/mL), Timo AIII (2 μM), or Timo AIII (2 μM) + VEGF (50 ng/mL) for another 48 h. HUVECs treated with 0.1% DMSO served as a vehicle control. The cell independence, expressed as the cell index, was recorded every hour.

Endothelial cell migration and invasion assay

The effects of Timo AIII on the migration and invasion of HUVECs were evaluated using a Matrigel (BD Biosciences, San Jose, CA, USA) transwell system with 24-well companion plates (8 μm pores). In the migration assay, HUVECs were directly seeded onto the upper side of the transwell. In each upper well, HUVECs were suspended in 200 μL basal F12-K medium at a cell density of 2.5×10^5 cells/mL that also containing VEGF (50 ng/mL) with or without various concentrations (0.5, 1, 2, and 4 μM) of Timo AIII. HUVECs were treated with 0.1% DMSO as a vehicle control and SU5416 as a positive control. After incubation for 24 h, HUVECs were removed using cotton swabs from the inner surface of the transwell insert. Then, the HUVECs on the outside of the transwell insert were fixed with 4% paraformaldehyde for 15 min at room temperature (RT) and stained with Hoechst 33342 (10 μg/mL) for 15 min. The membranes were washed with PBS and mounted on microscope slides. HUVECs were excited with UV light and captured at 4 × magnification under a fluorescent inverted microscope. In the invasion assay, the upper and lower sides of the membrane were precoated with Matrigel. The drug treatment and observation methods for the following invasion assay were the same as those for the migration assay. The cell migration and invasion ability of HUVECs were evaluated by ImageJ to quantify the cell number in each field.

Endothelial cell tube formation assay

The tube formation assay was performed using a μ-Slide Angiogenesis system coated with Matrigel. HUVECs were suspended in 50 μL basal F-12K medium at a density of 2.5×10^5 cells/mL that also contained VEGF (50 ng/mL) with or without various concentrations of Timo AIII (0.5, 1, 2, and 4 μM). HUVECs were treated with 0.1% DMSO as a vehicle control and SU5416 as a positive control. After 6 h of incubation, the cells were imaged at ×4 magnification under an inverted microscope. The number of loop formations was counted in each field.

Western blotting analysis

HUVECs were incubated with various concentrations (0.5, 1, and 2 μM) of Timo AIII for 24 h. HUVECs were treated with 0.1% DMSO as a vehicle control. After drug treatment, HUVECs were washed with ice-cold PBS three times and lysed in lysis buffer containing 0.5 M NaCl, 50 mM Tris, 1 mM EDTA, 0.05% SDS, 0.5% Triton X-100, and 1 mM PMSF. Cell lysates were centrifuged at 12 000 × *g* for 15 min at 4 °C. The protein concentration was measured using a BCA assay kit (Pierce, Rockford, IL, USA). Then, protein was denatured with loading buffer, and 30 μg of total protein from each sample was separated by SDS-PAGE and transferred to a polyvinylidene fluoride (0.45 μm) membrane, which was blocked with 5% BSA. Immunoblots were incubated with primary antibodies, including antibodies against VEGFR 1 (1:500, CST), phospho-VEGFR 2 (1:500, CST), VEGFR 2 (1:500, CST), phospho-Akt (1:1000, CST), Akt (1:1000,

CST), phospho-ERK1/2 (1:1000, CST), ERK1/2 (1:1000, CST), phospho-MEK1/2 (1:1000, CST), MEK1/2 (1:1000, CST), phospho-P38 MAPK (1:1000, CST), P38 MAPK (1:1000, CST), or GAPDH (1:2000, CST), at 4 °C overnight. After washing with TBST three times, the immunoblots were incubated with horseradish peroxidase-conjugated goat anti-rabbit IgG (1:2000, CST) for 2 h at RT. After the final wash, the immunoblots were visualized using an enhanced ECL system (Beyotime BeyoECL moon, Shanghai, China). The membranes were then imaged on an imaging system (GE AM600, Fairfield, CT, USA), and the intensity of each protein band was analyzed by ImageJ.

RNA-Seq and data analysis

RNA-Seq was performed with the Sequencing Platform BGISEQ-500 (BGI, Shenzhen, China). Briefly, HUVEC cells or Tübingen (TU) strain zebrafish embryos (1 dpf) were treated with various concentrations of Timo AIII for 24 h. Then, the HUVEC cells and zebrafish embryos were harvested, with three and four repetitive samples per group, respectively. The total RNA of each sample was extracted, and a sequencing library was constructed. The SOAPnuke analysis tool (v1.5.2, -l 15 -q 0.2 -n 0.05) was used to analyze the sequence quality and filter low-quality reads with quality scores lower than 20. HISAT2 (v2.0.4) was used to map the clean reads to the reference genome (Homo Sapiens: UCSC_hg38; Danio rerio: NCBI_GRCz11). Then, the clean reads were mapped to the reference transcript by Bowtie2 (v2.2.5), and the expression values were calculated by RSEM (v1.2.12). DEGseq (parameter: fold change ≥ 2 and adjusted P value < 0.001) was used to identify differentially expressed genes (DEGs) between the control and treatment groups. The transcript level was calculated according to the fragments per kilobase of transcript per million mapped reads (FPKM). For gene ontology (GO) analysis of the DEGs, the GO annotation results were classified into official classifications, including molecular function, cellular component, and biological

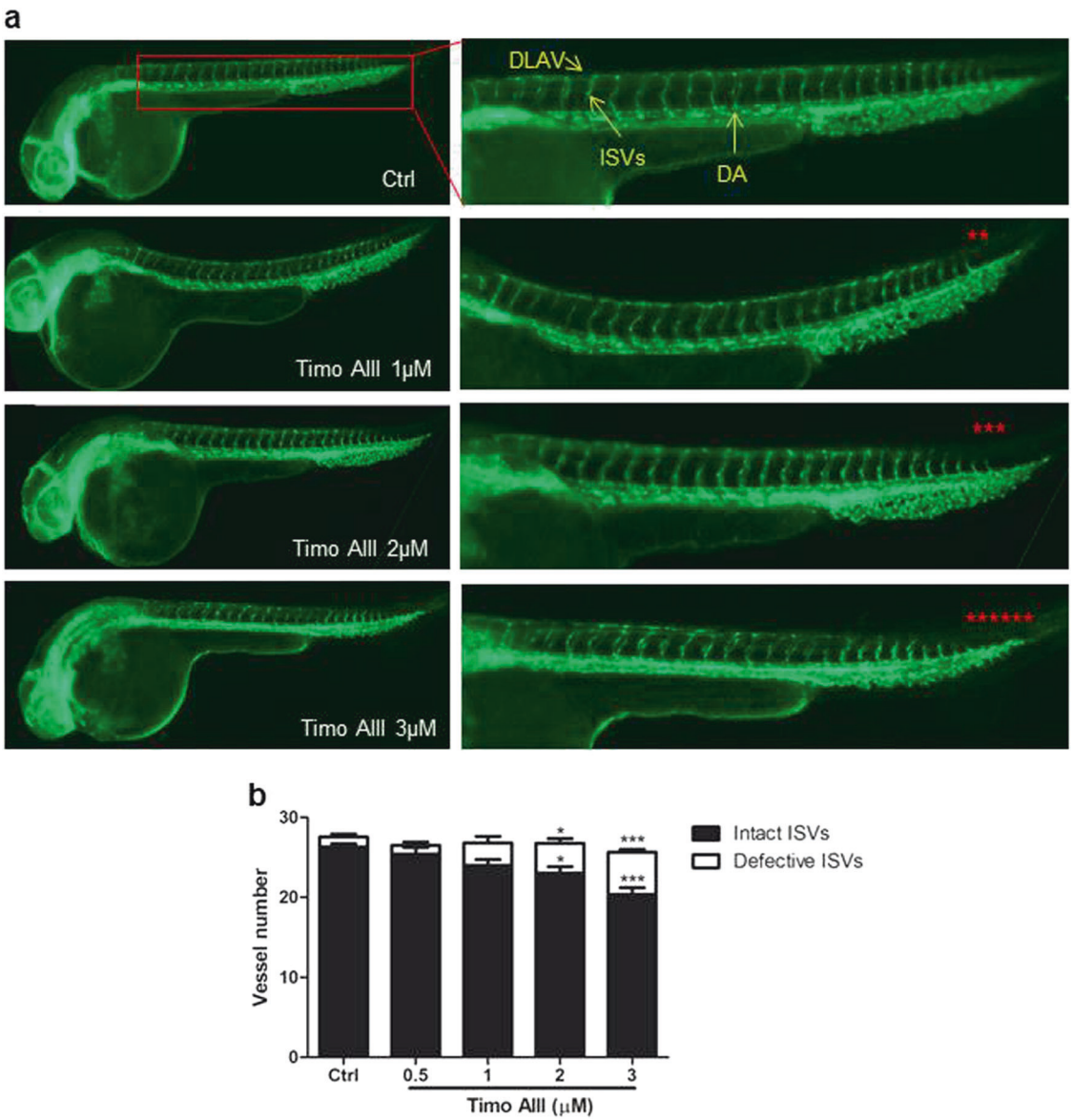

Fig. 2 Timo AIII inhibits ISVs growth in zebrafish. **a** Transgenic zebrafish Tg(*fli-1a*: EGFP)^{y1} expressed EGFP in endothelial cells, and the vessels were easily observed under a microscope. Twenty-four hpf (hour post fertilization) zebrafish embryos were treated with various concentrations of Timo AIII (0.5, 1, 2, and 3 μM) for 12 h and then imaged under an inverted microscope. Red asterisks indicate defective ISVs. **b** The statistical graph indicates the intact and defective vessel numbers of ISVs in zebrafish. The results are presented as the means ± S.E.M. *P < 0.05 and ***P < 0.001 versus the control group

process. The R package function phyper was used to perform GO enrichment analysis of DEGs. The false discovery rate (FDR) was calculated for each P value, and FDR < 0.01 was defined as significantly enriched. The same method was used to annotate and enrich the results of the KEGG metabolic pathway analysis of the DEGs. Coexpression network analysis based on the gene expression profile was conducted using the R package WGCDNA.

Statistical analysis

Data are presented as the mean ± S.E.M. from at least three independent experiments. Student's t-test and analysis of variance were used to perform statistical evaluations of the differences between the two groups, and $P < 0.05$ was considered significant.

RESULTS

Timosaponin AIII inhibited intersegmental vessels and subintestinal vessels growth in zebrafish

The transgenic zebrafish line Tg(*fli-1a*: EGFP)^{y1}, which expresses EGFP in endothelial cells [25], was employed to test the effect of Timo AIII on antiangiogenesis. Twenty-four hpf (hours post fertilization) zebrafish embryos were treated with various concentrations of Timo AIII for 12 h, and we found that Timo AIII inhibited intersegmental vessels (ISVs) growth in the tail of zebrafish (Fig. 2a). Statistical graphs indicated that Timo AIII dose-dependently decreased the intact vessel number and increased the defective vessel number of ISVs (Fig. 2b). Consistently, the growth of subintestinal vessels (SIVs) was also inhibited after treatment with Timo AIII for 48 h (Fig. 3a). Timo AIII also decreased the total area of SIVs (Fig. 3b). These data indicated that Timo AIII had an antiangiogenic effect in zebrafish.

Timo AIII suppressed endothelial cell proliferation in HUVECs

Endothelial cell proliferation initiates angiogenesis [26]. To detect the effect of Timo AIII on endothelial proliferation, we employed HUVECs as our experimental model. We found that Timo AIII concentration-dependently decreased cell viability and was cytotoxic in HUVECs (Figs. 4a and S1). Cell viability was significantly decreased at concentrations of 4 and 8 μM, while there was no cytotoxicity over the concentration range of ≤2 μM. In addition, Timo AIII inhibited VEGF-induced cell proliferation at concentrations of 1, 2, and 4 μM (Fig. 4b). Consistently, we also found that Timo AIII suppressed VEGF-induced endothelial cell proliferation using an RTCA system (Fig. 4c). HUVECs were treated with the selective VEGF receptor (VEGFR) inhibitor SU5416 as a positive control. These results revealed that Timo AIII significantly inhibited endothelial cell proliferation.

Timo AIII inhibited VEGF-induced endothelial cell migration in HUVECs

The migration of HUVECs was evaluated by a classical transwell assay [27]. HUVECs treated with VEGF significantly increased the number of migrated cells, while cotreatment with Timo AIII and VEGF reduced the number of migrated cells in a concentration-dependent manner (Fig. 5a, b). HUVECs were treated with SU5416, a VEGFR2 inhibitor that served as a positive control. HUVECs were stained with the nuclear indicator Hoechst for easy observation. As shown in Figs. 4a and S1, Timo AIII was not toxic to HUVECs over

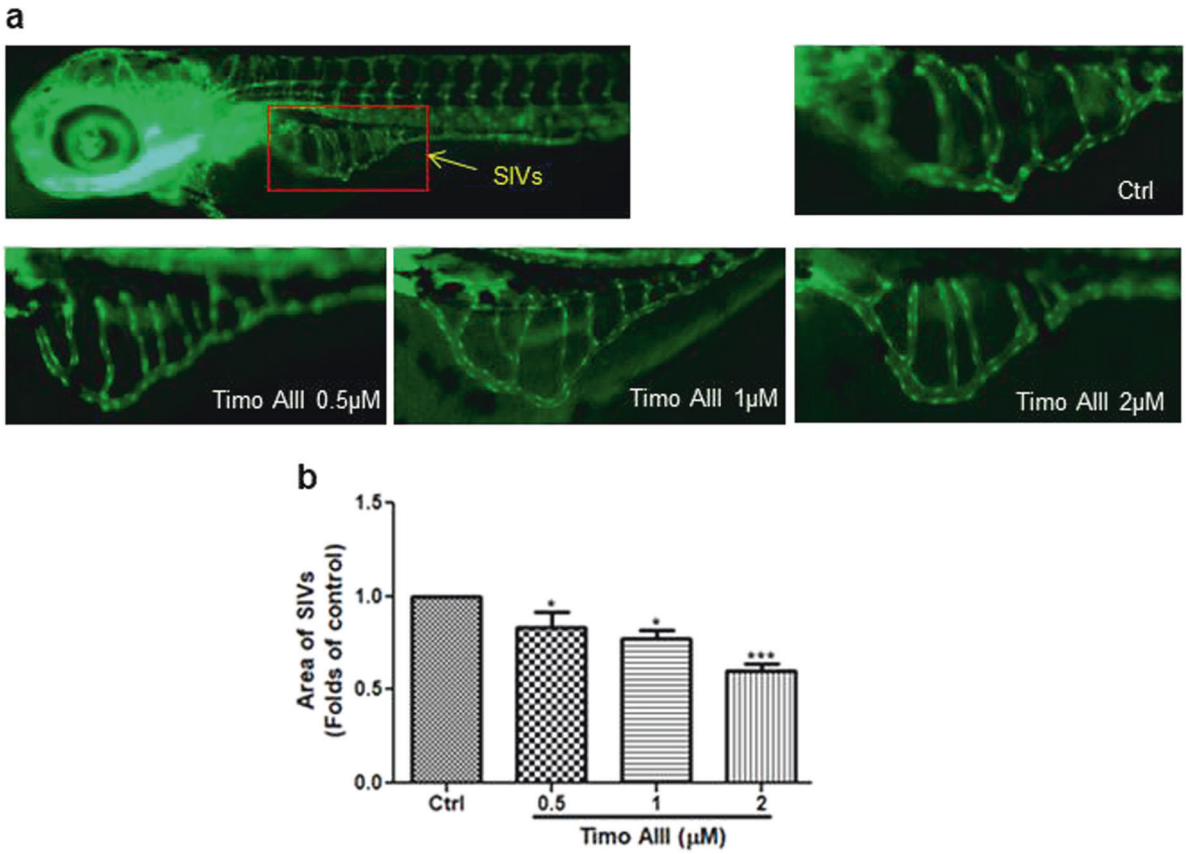

Fig. 3 Timo AIII inhibits SIVs growth in zebrafish. **a** Twenty-four hpf (hours post fertilization) zebrafish embryos were treated with various concentrations of Timo AIII (0.5, 1, and 2 μM) for 48 h; and then, the SIVs were imaged under an inverted microscope. Zebrafish incubated with 0.1% DMSO served as a vehicle control. **b** The total area of SIVs was analyzed by ImageJ, and the data are expressed as folds of the control. The results are presented as the means ± S.E.M. *$P < 0.05$ and ***$P < 0.001$ versus the control group

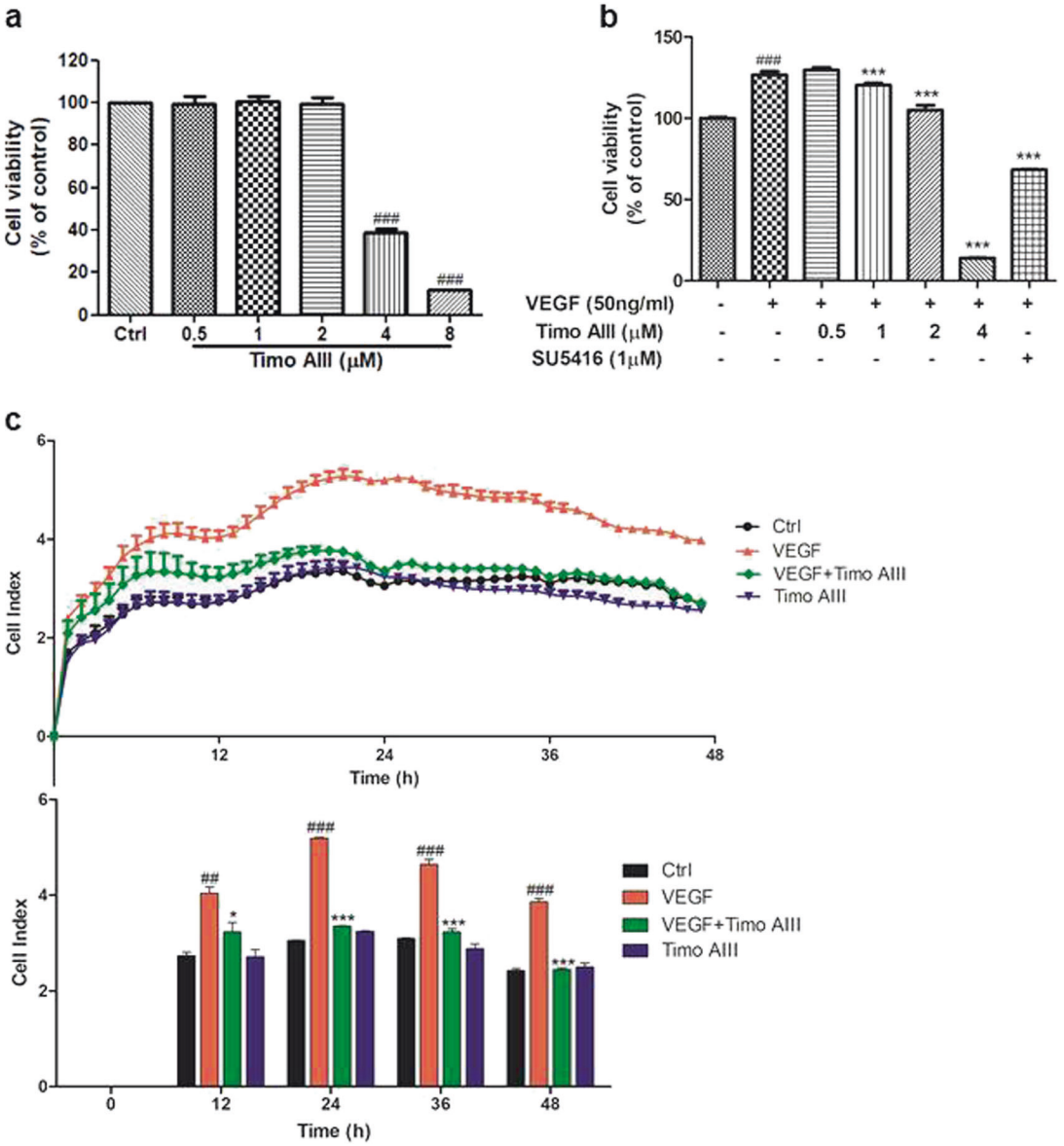

Fig. 4 Timo AIII inhibits endothelial cell proliferation in HUVECs. **a** HUVECs were treated with various concentrations of Timo AIII (0.5, 1, 2, 4, and 8 μM) for 24 h, and cell viability was tested by the MTT assay. **b** HUVEC cells were cotreated with VEGF (50 ng/mL) and various concentrations of Timo AIII (0.5, 1, 2, and 4 μM) or SU5416 (1 μM), which served as a positive control, for 24 h, and cell viability was determined by the MTT assay. **c** Cell impedance, which was expressed as the cell index and measured by the xCELLigence Real-time cell analysis (RTCA) system, was used to evaluate the proliferation in HUVECs. HUVECs were treated with VEGF (50 ng/mL), Timo AIII (2 μM), or VEGF (50 ng/mL) + Timo AIII (2 μM) for 48 h, and cell impedance was detected at 1-h intervals. Data are presented as the percentage of the control group. The results are presented as the means ± S.E.M. $^{\#\#}P < 0.01$ and $^{\#\#\#}P < 0.001$ versus the control group. $^{*}P < 0.05$, $^{***}P < 0.001$ versus the VEGF-treated group

the concentration range of 0.5–2 μM. These results indicated that Timo AIII suppressed VEGF-induced endothelial cell migration and that the cell migration inhibitory effect of Timo AIII was not associated with its cytotoxicity.

Timo AIII attenuated VEGF-induced endothelial cell invasion in HUVECs

Invasion plays vital roles in both tumor angiogenesis and metastasis [28, 29]. The invasion ability of HUVECs was determined according to the amount of cells that passed through the Matrigel and membrane barriers in a transwell system. As shown in Fig. 6a, b, VEGF significantly enhanced the invasion cell number of HUVECs and Timo AIII obviously suppressed the invasion cell number under nontoxic concentrations in a dose-dependent manner. HUVECs were incubated with SU5416 as a positive control. These results suggested that Timo AIII attenuated VEGF-induced invasion in HUVECs.

Timo AIII reduced VEGF-induced tube formation in HUVECs

An endothelial cell tube formation assay was used to mimic the process of neovascularization. In the present study, we found that VEGF increased the loop number of the network tube structure of HUVECs, while Timo AIII dramatically inhibited the loop number in each field (Fig. 7a, b). HUVECs were incubated with SU5416 as a positive control. In this experiment, HUVECs were also treated with Timo AIII at nontoxic concentrations from 0.5 to 2 μM (Figs. 4a and S1), and Timo AIII reduced VEGF-induced tube formation in a concentration-dependent manner. We also tested the effects of

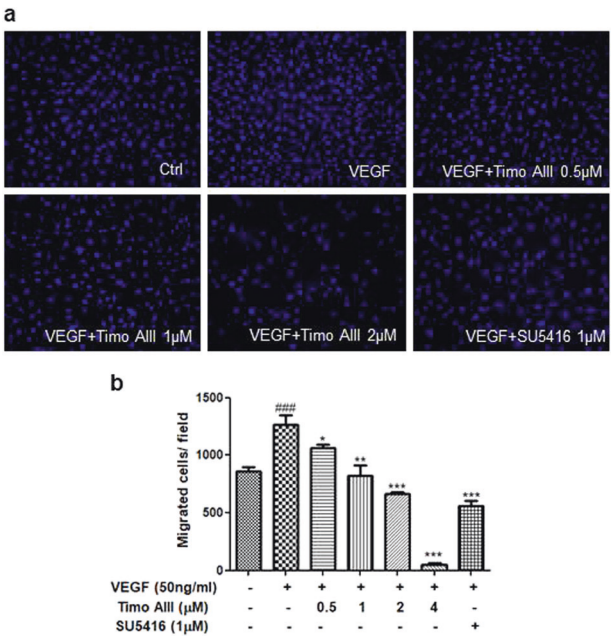

Fig. 5 Timo AIII inhibits VEGF-induced migration in HUVECs. The migration ability of HUVECs was measured by a classical transwell migration assay. **a** HUVECs were treated with VEGF (50 ng/mL) and various concentrations (0.5, 1, 2, and 4 μM) of Timo AIII for 24 h. HUVECs incubated with 0.1% DMSO served as a vehicle control and with SU5416 (1 μM) as a positive control. The nuclei of HUVECs were stained with Hoechst 33342 and produced blue fluorescence when excited by the UV light. Representative images show the migration ability of HUVECs under the different treatment conditions. **b** The statistical graph shows the quantitative analysis of HUVEC migration. Data are presented as the cell number per field. The results are presented as the means ± S.E.M. $^{###}P < 0.001$ versus the control group; $^{*}P < 0.05$, $^{**}P < 0.01$, and $^{***}P < 0.001$ versus the VEGF-treated group

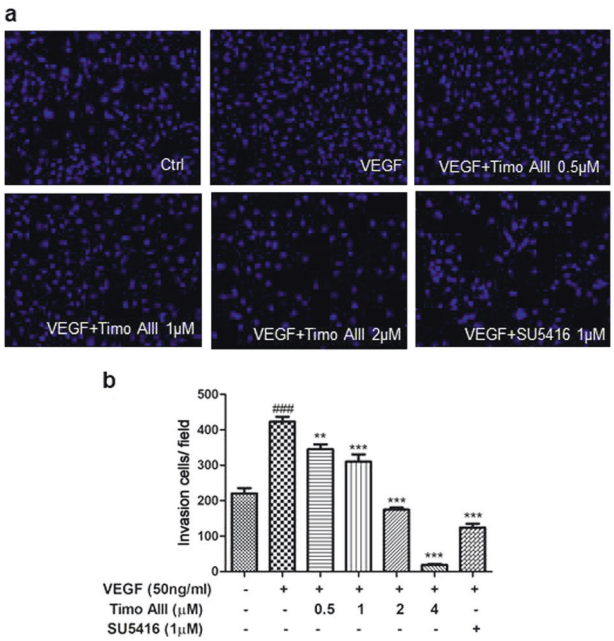

Fig. 6 Timo AIII inhibits VEGF-induced invasion in HUVECs. The invasion ability of HUVECs was measured by a transwell system coated with Matrigel. **a** HUVECs were treated with VEGF (50 ng/mL) and various concentrations (0.5, 1, 2, and 4 μM) of Timo AIII for 24 h. HUVECs incubated with 0.1% DMSO served as a vehicle control and with SU5416 (1 μM) as a positive control. HUVECs were stained with Hoechst 33342. Representative images show the invasion ability of HUVECs under different treatment conditions. **b** The statistical graph shows the quantitative analysis of HUVEC invasion. Data are presented as the cell number per field. The results are presented as the means ± S.E.M. $^{###}P < 0.001$ versus the control group; $^{**}P < 0.01$ and $^{***}P < 0.001$ versus the VEGF-treated group

VEGF and Timo AIII on cell proliferation during the tube formation process and found that VEGF treatment with or without Timo AIII did not significantly affect the cell proliferation of HUVECs after incubation for 6 h (Fig. 7c). Therefore, we concluded that the tube formation inhibitory effect of Timo AIII was not associated with its inhibition of VEGF-induced endothelial cell proliferation.

Timo AIII affected VEGF/PI3K/Akt/MAPK signaling in HUVECs

Endothelial cell proliferation, migration, and invasion are dramatically regulated by the VEGF/VEGFR/MAPK signaling pathway [25, 30]. As shown from the Western blotting results presented in Fig. 8a, Timo AIII downregulated the protein levels of VEGFR 1 and 2. The phosphorylation levels of Akt, MEK1/2, and ERK1/2 were attenuated by treatment with Timo AIII, while the phosphorylation levels of P38 and JNK were not significantly changed (Fig. 8b–f). Timo AIII also decreased the expression of JNK (Fig. 8d). In addition, Timo AIII suppressed the phosphorylation of VEGFR2, Akt, and ERK1/2 triggered by VEGF (Fig. 9a–c). These results suggested that the underlying mechanism of the antiangiogenic effect of Timo AIII might be related to the inhibition of the VEGF/PI3K/Akt/MAPK signaling pathway.

Transcriptome analysis of Timo AIII-regulated gene expression in HUVECs and zebrafish embryos

To further clarify the underlying mechanism of the antiangiogenesis effect of Timo AIII, we conducted RNA-Seq to examine the genome-wide transcriptional changes between the Timo AIII-treated group and the control group in both HUVECs and TU strain zebrafish embryos. The DEGs between the control group and the Timo AIII-treatment group were identified in both HUVEC cells and zebrafish. In addition, we performed coexpression network analysis based on the expression profile normalized by the FPKM using the R package WGCDNA. Network analysis indicated that 30 and 33 modules were constructed in Timo AIII-treated HUVEC cells (Fig. S4a) and zebrafish (Fig. S4b), respectively. Among them, we detected many significant trait-related modules (Fig. S4a, b). GO and KEGG enrichment analyses of the highly connected genes in these trait-related modules demonstrated that many processes and pathways were significantly enriched, including angiogenesis, cell motility, cell adhesion, protein serine/threonine kinase activity, transmembrane signaling receptor activity, growth factor activity, etc. (Fig. S4c–e). These findings were consistent with our experimental results that showed Timo AIII inhibited angiogenesis in endothelial cells and zebrafish.

DISCUSSION

The present study explored the antiangiogenesis effect of Timo AIII (Fig. 1) on HUVECs in vitro and zebrafish in vivo. In zebrafish, we found that Timo AIII inhibited the growth of ISVs and SIVs in a concentration-dependent manner. In HUVECs, we demonstrated that Timo AIII attenuated cell proliferation, migration, invasion, and tube formation. The underlying mechanism might involve the VEGF/PI3K/Akt/MAPK signaling pathway. This study was the first to investigate the potential antiangiogenic properties of Timo AIII.

Angiogenesis plays vital roles in tumor growth and metastasis. Timo AIII was proposed to be a potential natural compound for

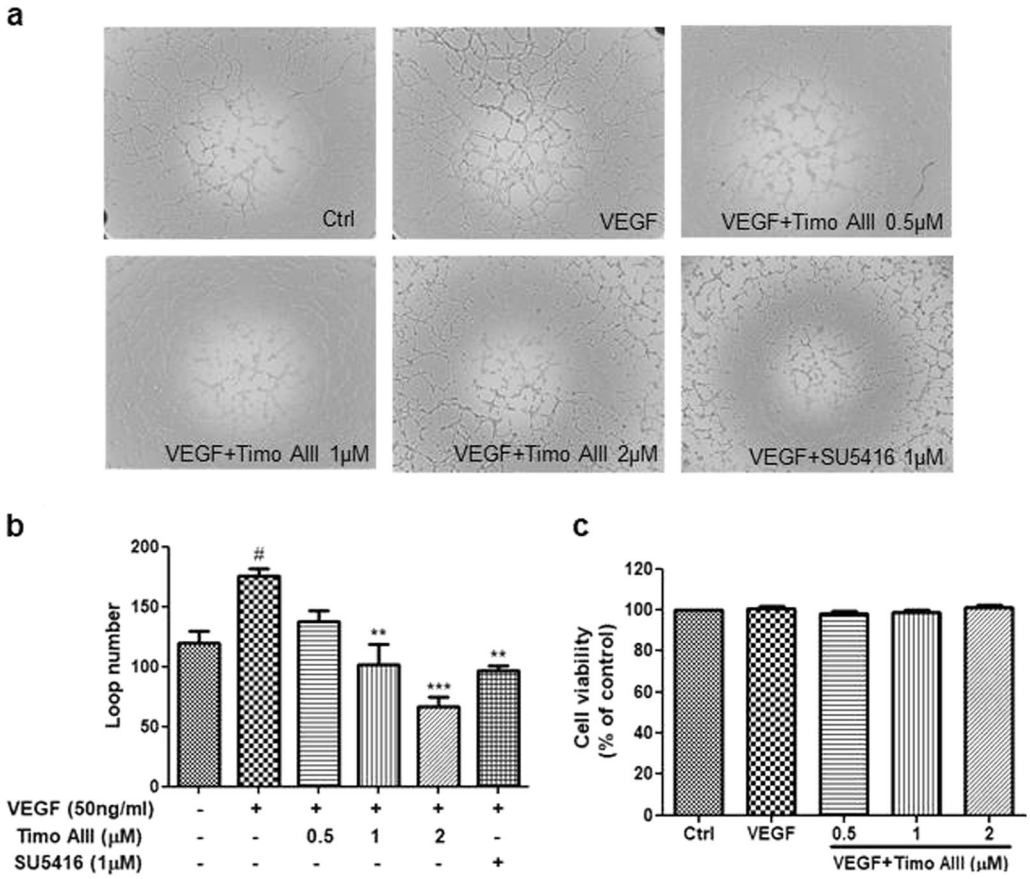

Fig. 7 Timo AIII inhibits endothelial cell tube formation in HUVECs. The tube formation ability of HUVECs was examined by a μ-Slide coated with Matrigel. **a** HUVECs were treated with VEGF (50 ng/mL) and various concentrations (0.5, 1, and 2 μM) of Timo AIII for 6 h. HUVECs incubated with 0.1% DMSO served as a vehicle control and with SU5416 (1 μM) as a positive control. HUVECs were imaged under an inverted microscope. Representative images show the tube formation ability of HUVECs under different treatment conditions. **b** The statistical graph shows the quantitative analysis of HUVEC tube formation. Data are presented as the loop number per field. **c** HUVECs were treated with VEGF (50 ng/mL) and various concentrations (0.5, 1, and 2 μM) of Timo AIII for 6 h. Cell viability was tested by the MTT assay. The results are presented as the means ± S.E.M. $^{\#}P < 0.05$ versus the control group; $^{**}P < 0.01$ and $^{***}P < 0.001$ versus the VEGF-treated group

anticancer drug development in recent studies [14]. Although the anticancer effect of Timo AIII has been demonstrated in various types of cancers, the antiangiogenesis effect of Timo AIII has not been elucidated. In our previous studies, our group established the transgenic zebrafish line Tg(*fli-1a*: EGFP)^{y1} and HUVECs as effective models for antiangiogenesis compound screening and studying its underlying mechanism [25, 30]. In the present study, we found that Timo AIII inhibited ISVs and SIVs growth in zebrafish embryos in a dose-dependent manner (Figs. 2 and 3). These results provide evidence for the antiangiogenesis effect of Timo AIII in vivo.

In previous studies, Timo AIII inhibited cell proliferation, migration, and invasion at concentrations of 1, 3, 6, and 9 μM in the lung cancer cell line A549 [16]. Timo AIII suppressed the metastasis of renal carcinoma cells at concentrations of 4, 6, and 10 μM [31]. Timo AIII attenuated the oncogenic phenotype of breast cancer cells at concentrations of 2 and 4 μM [32]. Thus, the concentrations of Timo AIII used in the anticancer studies varied depending on the cancer types and experimental conditions.

Endothelial cells play critical roles in vascular functions, including angiogenesis [26, 33, 34]. Endothelial cell proliferation initiated the growth of new blood vessels, and Timo AIII inhibited the proliferation of HUVECs (Fig. 4a). VEGF is an angiogenesis driver and plays a vital role in the process of tumor angiogenesis [30]. Timo AIII reduced VEGF-induced endothelial cell proliferation in HUVECs regardless of its cytotoxicity (Fig. 4b). Consistently, an RTCA system, which can detect the impendence of attached cells, also indicated real-time inhibition of endothelial cell proliferation by Timo AIII (Fig. 4c). In addition, endothelial cell migration and invasion were detected by a classic transwell system. We found that Timo AIII suppressed VEGF-induced endothelial cell migration and invasion in HUVECs over the range of nontoxic concentrations of Timo AIII (Figs. 5 and 6). These results were consistent with the antiproliferation, antimigration, and antiinvasion effects of Timo AIII found in various types of cancer cells [16, 20]. The tube formation of endothelial cells, which mimicked 3-D network vascular growth, was measured by an easily operated μ-Slide coated with Matrigel. Timo AIII disrupted the tube formation of HUVECs (Fig. 7a, b), while Timo AIII and VEGF did not affect cell proliferation in HUVECs (Fig. 7c). HUVECs treated with the specific VEGFR inhibitor SU5416 served as positive controls in these experiments. Thus, we concluded that Timo AIII reduced endothelial cell proliferation, migration, invasion, and tube formation and had an antiangiogenic effect in HUVECs in vitro. However, Timo AIII was not cytotoxic and did not affect cell apoptosis or the cell cycle in HUVECs (Fig. S2 and Table S1). We also tested the cytotoxicity of Timo AIII on the rat aortic smooth muscle cell line A7r5 and found that Timo AIII did not significantly inhibit cell proliferation at concentrations of 0.5, 1, and 2 μM (Fig. S3).

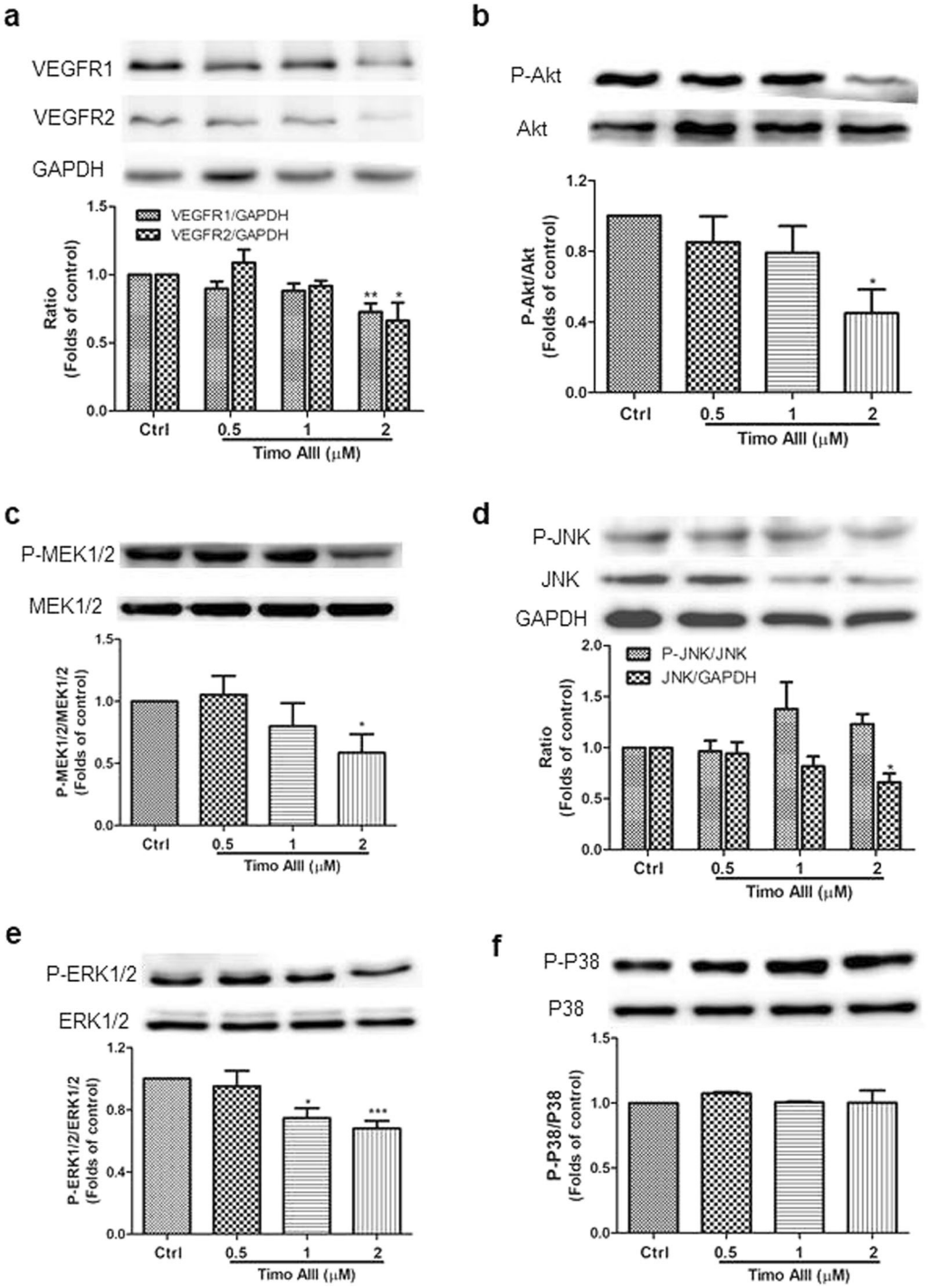

Fig. 8 Timo AIII attenuates the VEGF/PI3K/Akt/MAPK signaling pathway in HUVECs. **a–f** HUVECs were treated with various concentrations of Timo AIII (0.5, 1, and 2 μM) for 24 h. HUVECs incubated with 0.1% DMSO served as a vehicle control. Phosphorylated and total proteins were detected by Western blotting using the specific antibodies. The ratio of phosphorylated and total proteins was calculated. Data are presented as the fold of the control group. The results are presented as the means ± S.E.M. *$P < 0.05$, **$P < 0.01$, and ***$P < 0.001$ versus the control group

These results were consistent with the results in endothelial cell HUVECs.

Previous studies revealed that Timo AIII induced apoptosis though the activation of the caspase cascade via the JNK1/2 pathway [23]. Timo AIII reduced hepatocyte growth factor-induced invasion by ERK inhibition in a breast cancer cell line [20]. Thus, the MAPK signaling pathway might also be recruited in mechanism of the antiangiogenesis effect of Timo AIII in endothelial cells. Furthermore, activation of MAPK signaling mediated by VEGF and VEGFR is an essential mechanism in angiogenesis [25]. In this study, Timo AIII downregulated the protein levels of VEGFR 1 and 2 (Fig. 8a). Timo AIII suppressed the phosphorylation of Akt, MEK1/2, and ERK1/2 but not P38 and JNK in HUVECs (Fig. 8b–f). Timo AIII also decreased the expression of JNK (Fig. 8d). Moreover, VEGF stimulated the phosphorylation of VEGFR2, Akt, and ERK1/2, and Timo AIII also attenuated these processes (Fig. 9a–c). Cotreatment with Timo AIII

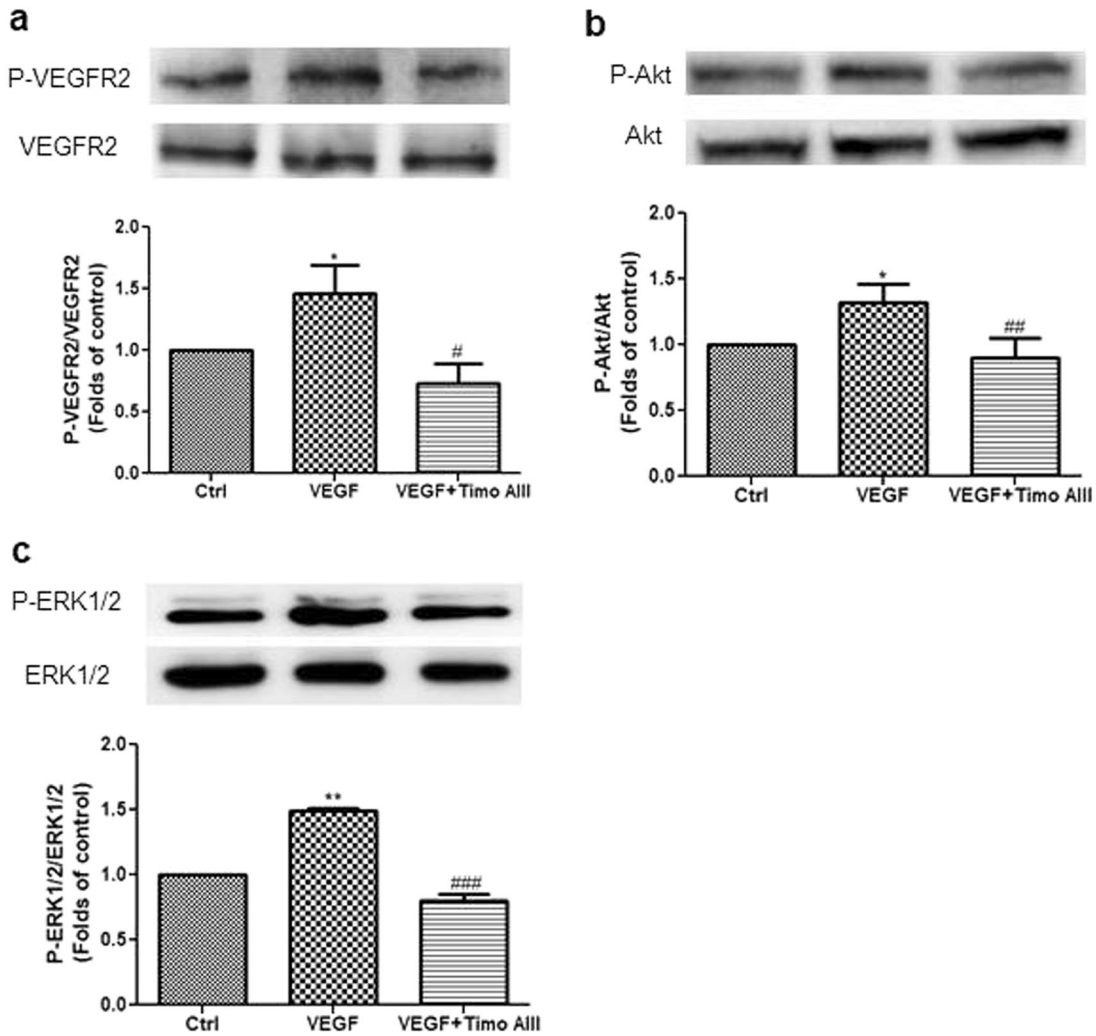

Fig. 9 Timo AIII suppresses the VEGF-activated VEGF/PI3K/Akt/MAPK signaling pathway in HUVECs. **a–c** HUVECs were treated with VEGF (50 ng/mL) with or without Timo AIII (2 μM) for 24 h. HUVECs incubated with 0.1% DMSO served as a vehicle control. Phosphorylated and total proteins were detected by Western blotting using the specific antibodies. The ratios of phosphorylated and total proteins were calculated. Data are presented as the fold of the control group. The results are presented as the means ± S.E.M. $^{*}P < 0.05$ and $^{**}P < 0.01$ versus the control group. $^{\#}P < 0.05$, $^{\#\#}P < 0.01$, and $^{\#\#\#}P < 0.001$ versus the VEGF-treated group

and VEGF did not decrease the expression of VEGFR2 (Fig. 9a), while treatment with Timo AIII alone decreased VEGFR2 expression (Fig. 8a) in HUVECs. These results might be due to the complicated regulation of VEGF in endothelial cells. These results revealed that Timo AIII inhibited the VEGF/PI3K/Akt/MAPK signaling pathway in endothelial cells, which might be the underlying mechanism of the antiangiogenesis effect of Timo AIII. In addition, the transcriptome data indicated that several cellular processes and pathways, including angiogenesis, cell motility, cell adhesion, protein serine/threonine kinase activity, transmembrane signaling receptor activity, and growth factor activity, were related to the treatment of HUVECs and zebrafish embryos with Timo AIII (Fig. S4). These results further confirmed the antiangiogenesis effect of Timo AIII.

CONCLUSION

In summary, Timo AIII partially disrupted SIVs and ISVs growth in zebrafish embryos. Timo AIII inhibited endothelial cell proliferation, migration, invasion, and tube formation in HUVECs. The underlying mechanism of the antiangiogenesis effect of Timo AIII might be involved in the inhibition of the VEGF/PI3K/Akt/MAPK signaling pathway. For the first time, we demonstrated the antiangiogenesis effect of Timo AIII in HUVECs in vitro and zebrafish in vivo.

ACKNOWLEDGEMENTS

This study was supported by the Shanghai University of Traditional Chinese Medicine (A1-U17205010301), the National Health Commission of Shanghai (GWIV-28, ZY-(2018-2020)-FWTX-8001), and the National Natural Science Foundation of China (81603549, 81673726, and 81760860)

AUTHOR CONTRIBUTIONS

ZYZ conducted the experiments and wrote the manuscript. WRZ and YX conducted the experiments and analyzed the data. CH analyzed the transcriptome data. XMZ, WTS, and JZ conducted the experiments. QY and XLC designed the study. JYT designed the study and revised the manuscript.

ADDITIONAL INFORMATION

The online version of this article (https://doi.org/10.1038/s41401-019-0291-z) contains supplementary material, which is available to authorized users.

Competing interests: The authors declare no competing interests.

REFERENCES

1. Siegel RL, Miller KD, Jemal A. Cancer statistics, 2017. CA Cancer J Clin. 2017;67:7–30.
2. Zheng R, Zeng H, Zhang S, Chen W. Estimates of cancer incidence and mortality in China, 2013. Chin J Cancer. 2017;36:66.
3. Mashreghi M, Azarpara H, Bazaz MR, Jafari A, Masoudifar A, Mirzaei H, et al. Angiogenesis biomarkers and their targeting ligands as potential targets for tumor angiogenesis. J Cell Physiol. 2018;233:2949–65.
4. Folkman J. Tumor angiogenesis: therapeutic implications. N Engl J Med. 1971;285:1182–6.
5. Cook KM, Figg WD. Angiogenesis inhibitors: current strategies and future prospects. CA Cancer J Clin. 2010;60:222–43.
6. Sakamoto S, Ryan AJ, Kyprianou N. Targeting vasculature in urologic tumors: mechanistic and therapeutic significance. J Cell Biochem. 2008;103:691–708.
7. Hoff PM, Machado KK. Role of angiogenesis in the pathogenesis of cancer. Cancer Treat Rev. 2012;38:825–33.
8. Lee B, Jung K, Kim DH. Timosaponin AIII, a saponin isolated from *Anemarrhena asphodeloides*, ameliorates learning and memory deficits in mice. Pharmacol Biochem Behav. 2009;93:121–7.
9. Wang Y, Dan Y, Yang D, Hu Y, Zhang L, Zhang C, et al. The genus *Anemarrhena Bunge*: a review on ethnopharmacology, phytochemistry and pharmacology. J Ethnopharmacol. 2014;153:42–60.
10. Lim SM, Jeong JJ, Kang GD, Kim KA, Choi HS, Kim DH. Timosaponin AIII and its metabolite sarsasapogenin ameliorate colitis in mice by inhibiting NF-κB and MAPK activation and restoring Th17/Treg cell balance. Int Immunopharmacol. 2015;25:493–503.
11. Cong Y, Wang L, Peng R, Zhao Y, Bai F, Yang C, et al. Timosaponin AIII induces antiplatelet and antithrombotic activity via Gq-mediated signaling by the thromboxane A2 receptor. Sci Rep. 2016;6:38757.
12. Lee B, Trinh HT, Jung K, Han SJ, Kim DH. Inhibitory effects of steroidal timosaponins isolated from the rhizomes of *Anemarrhena asphodeloides* against passive cutaneous anaphylaxis reaction and pruritus. Immunopharmacol Immunotoxicol. 2010;32:357–63.
13. Wu ZT, Qi XM, Sheng JJ, Ma LI, Ni X, Ren J, et al. Timosaponin A3 induces hepatotoxicity in rats through inducing oxidative stress and down-regulating bile acid transporters. Acta Pharmacol Sin. 2014;35:1188–98.
14. Han FY, Song XY, Chen JJ, Yao GD, Song SJ. Timosaponin AIII: a novel potential anti-tumor compound from *Anemarrhena asphodeloides*. Steroids. 2018;140:125–30.
15. King FW, Fong S, Griffin C, Shoemaker M, Staub R, Zhang Y-L, et al. Timosaponin AIII is preferentially cytotoxic to tumor cells through inhibition of mTOR and induction of ER stress. PLoS One. 2009;4:e7283.
16. Jung O, Lee J, Lee YJ, Yun JM, Son YJ, Cho JY, et al. Timosaponin AIII inhibits migration and invasion of A549 human non-small-cell lung cancer cells via attenuations of MMP-2 and MMP-9 by inhibitions of ERK1/2, Src/FAK and β-catenin signaling pathways. Bioorg Med Chem Lett. 2016;26:3963–7.
17. MarElia CB, Sharp AE, Shemwell TA, Clare Zhang Y, Burkhardt BR. *Anemarrhena asphodeloides* Bunge and its constituent timosaponin-AIII induce cell cycle arrest and apoptosis in pancreatic cancer cells. FEBS Open Bio. 2018;8:1155–66.
18. Wang Y, Xu L, Lou LL, Song SJ, Yao GD, Ge MY, et al. Timosaponin AIII induces apoptosis and autophagy in human melanoma A375-S2 cells. Arch Pharm Res. 2017;40:69–78.
19. Kim KM, Im AR, Kim SH, Hyun JW, Chae S. Timosaponin AIII inhibits melanoma cell migration by suppressing COX-2 and in vivo tumor metastasis. Cancer Sci. 2016;107:181–8.
20. Tsai CH, Yang CW, Wang JY, Tsai YF, Tseng LM, King KL, et al. Timosaponin AIII suppresses hepatocyte growth factor-induced invasive activity through sustained ERK activation in breast cancer MDA-MB-231 cells. J Evid Based Integr Med. 2013;2013:421051.
21. Wang N, Feng Y, Zhu M, Siu FM, Ng KM, Che CM. A novel mechanism of XIAP degradation induced by timosaponin AIII in hepatocellular carcinoma. Biochim Biophys Acta Mol Cell Res. 2013;1833:2890–9.
22. Kang YJ, Chung HJ, Nam JW, Park HJ, Seo EK, Kim YS, et al. Cytotoxic and antineoplastic activity of timosaponin A-III for human colon cancer cells. J Nat Prod. 2011;74:701–6.
23. Huang HL, Chiang WL, Hsiao PC, Chien MH, Chen HY, Weng WC, et al. Timosaponin AIII mediates caspase activation and induces apoptosis through JNK1/2 pathway in human promyelocytic leukemia cells. Tumour Biol. 2015;36:3489–97.
24. Chen JR, Jia XH, Wang H, Yi YJ, Wang JY, Li YJ. Timosaponin A-III reverses multidrug resistance in human chronic myelogenous leukemia K562/ADM cells via downregulation of MDR1 and MRP1 expression by inhibiting PI3K/Akt signaling pathway. Int J Oncol. 2016;48:2063–70.
25. Huang B, Peng Y, Li J, Li S, Sun Y, Wang D, et al. An andrographolide derivative AGP-26b exhibiting anti-angiogenic activity in HUVECs and zebrafish via blocking the VEGFA/VEGFR2 signaling pathway. Mol Omics. 2017;13:525–36.
26. Zhou ZY, Huan LY, Zhao WR, Tang N, Jin Y, Tang JY. Spatholobi Caulis extracts promote angiogenesis in HUVECs in vitro and in zebrafish embryos in vivo via up-regulation of VEGFRs. J Ethnopharmacol. 2017;200:74–83.
27. Zheng Y, Li Y, Liu G, Qi X, Cao X. MicroRNA-24 inhibits the proliferation and migration of endothelial cells in patients with atherosclerosis by targeting importin-α3 and regulating inflammatory responses. Exp Ther Med. 2018;15:338.
28. Paterson EK, Courtneidge SA. Invadosomes are coming: new insights into function and disease relevance. FEBS J. 2018;285:8–27.
29. Singh P, Jenkins LM, Horst B, Alers V, Pradhan S, Kaur P, et al. Inhibin is a novel paracrine factor for tumor angiogenesis and metastasis. Cancer Res. 2018;78:2978–89.
30. Zhong ZF, Hoi PM, Wu GS, Xu ZT, Tan W, Chen XP, et al. Anti-angiogenic effect of furanodiene on HUVECs in vitro and on zebrafish in vivo. J Ethnopharmacol. 2012;141:721–7.
31. Chiang KC, Lai CY, Chiou HL, Lin CL, Chen YS, Kao SH, et al. Timosaponin AIII inhibits metastasis of renal carcinoma cells through suppressing cathepsin C expression by AKT/miR-129-5p axis. J Cell Physiol. 2019;234:13332–41.
32. Gergely JE, Dorsey AE, Dimri GP, Dimri M. Timosaponin A-III inhibits oncogenic phenotype via regulation of PcG protein BMI1 in breast cancer cells. Mol Carcinog. 2018;57:831–41.
33. Zhou ZY, Xu JQ, Zhao WR, Chen XL, Jin Y, Tang N, et al. Ferulic acid relaxed rat aortic, small mesenteric and coronary arteries by blocking voltage-gated calcium channel and calcium desensitization via dephosphorylation of ERK1/2 and MYPT1. Eur J Pharmacol. 2017;815:26–32.
34. Zhou ZY, Zhao WR, Shi WT, Xiao Y, Ma ZL, Xue JG, et al. Endothelial-dependent and independent vascular relaxation effect of tetrahydropalmatine on rat aorta. Front Pharmacol. 2019;10:336.